Journal of the Ceramic Society of Japan 118 [4] 263-268 2010 Special Article
The 63th CerSJ Awards for Advancements in Ceramic Science and Technology: Review

Application of ion conductors for microfabrication of solid surface

Kai KAMADA†

Department of Materials Science and Engineering, Faculty of Engineering, Nagasaki University, 1–14 Bunkyo-machi, Nagasaki 852–8521

The present paper describes novel microfabrication techniques which utilize an ion migration at the microcontact between ion conductor and target solid. Two different methods have been recently proposed by our group. One is a solid state electrochemical route for pinpoint doping using an ion conductor. In this approach, an electric field is applied to the solid–solid interface between the cation conductor and target solid, inducing the injection of cations into the target. A significant advantage of this technique is that it enables pinpoint doping into desired locations within a solid target using the ion conductor having an extremely small contact area. On the other hand, we have also investigated an electrochemical microstructuring (i.e., micromachining) of metal surface through an anodic reaction of metal substrate attached to the needle-like ion conductor. The metal substrate is electrochemically oxidized, and then dissolves as M^{n+} into the ion conductor placed at the cathodic side. As a result of the continuous application of electric field, the metal surface is drilled according to the apex form of the ion conductor employed. This paper reveals the characteristics (merits and demerits) of the present techniques vis-a-vis conventional techniques for doping or micromachining.

Key-words : Solid electrolyte, Microelectrode, Microcontact, Pinpoint doping, Electrochemical micromachining

[Received November 9, 2009]

1. Introduction

Solid state ionics deals with fast ion migration in crystalline or non-crystalline solids under applying electric field or concentration gradient. Hence, solid materials possessing relatively high ionic conductivity, which are called ion conductors or solid electrolytes, are studied as targets in the physical, electrical, and chemical points of view. As well-known, the ion conductors (and/or mixed conductors) are applied for electrolytes or electrodes of electrochemical reactors such as sensors, batteries, etc. All devices utilizing ion conductor operate by either harvesting an electromotive force equivalent to the difference in the chemical potential of mobile ion on both sides of the ion conducting separator or transporting ions from one side to the other under an applied dc electric field.

In past decade, microcontact (microelectrodes) method, which is frequently applied for electrochemical measurements in solution system, has been widely used in the research field on solid state ionics.[1] Concretely, microcontacts play a significant role in the measurements of local conductivities in ceramic materials,[2] transference numbers in mixed conductors,[3),4] and in the determination of redox potentials in metal oxides.[5),6] The use of a microcontact allows a better control of electrochemical parameters and contact areas at the interface compared to a conventional planar electrode, which often shows time-dependent changes of the contact area because of its inhomogeneous interface.[7),8] On the other hand, our group has attempted to develop original microfabrication techniques using ion conductor with a small contact area, because more effective and finer-resolution machining and/or composition control technique is required due to recent demands for integration of micro-parts in state-of-the-art microsystems. We have investigated two different solid state microfabrication techniques through ion migration at the microcontact. One is the position-selective metal ion doping (**Fig. 1**),[9] where the positively charged metal ion in the conductor is injected into the desired position within a material under applying a dc bias. Micromachining belongs to the other category (**Fig. 2**),[10] can be realized as a result of local anodic

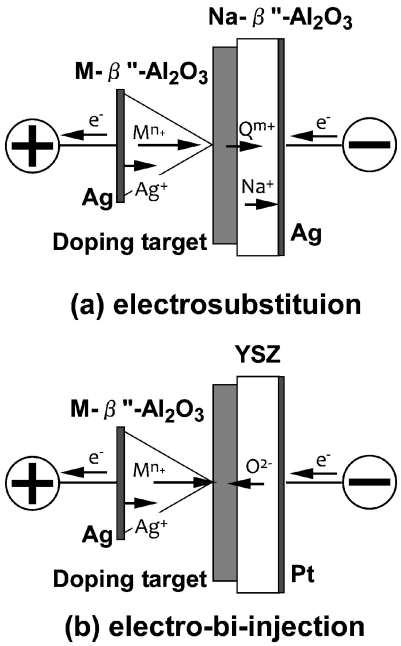

Fig. 1. Schematic ion migration models of pinpoint doping using pyramidal β''-Al_2O_3 ion conductor; (a) electrosubstitution and (b) electro-bi-injection.

† Corresponding author: K. Kamada; E-mail: kkamada@nagasaki-u.ac.jp

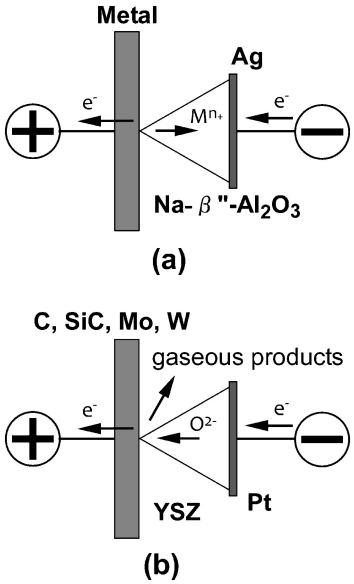

Fig. 2. Schematic system of solid state electrochemical micromachining using (a) metal ion and (b) oxide ion conductor.

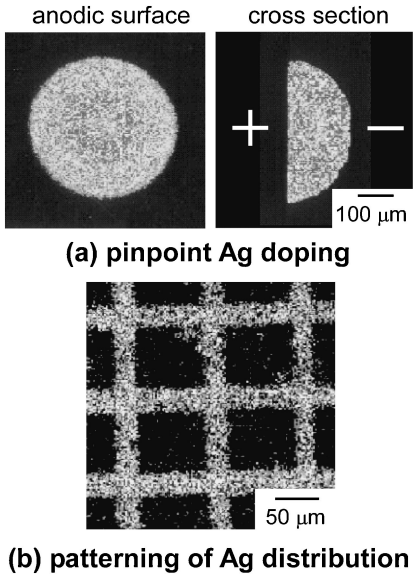

Fig. 3. (a) Elemental distribution maps of the anodic surface and cross section of Ag-doped glass after applying 10 μA for 1 h at 673 K. (b) Ag mapping sketched in the anodic glass surface by scanning Ag-β''-Al_2O_3 tip during pinpoint doping.

dissolution of metal substrate at the microcontact. Although a microcontact technique has already been used for the electrochemical measurements as stated above, it has merely been applied to microfabrication of solid surfaces within our knowledge.[11)–13)] Therefore, the present techniques are expected to grow as one of new applications of ion conductors in the near future. The following sections will focus on the fundamental mechanisms of the solid state microfabrication methods using ion conductors and present some experimental results.

2. Pinpoint doping using metal ion conductors

The physical and chemical properties of inorganic materials can be significantly modified by minute changes in the composition. Doping is a technique used to achieve this, which is the mixing the small amounts of different elements into the matrix, to modify properties. There are two approaches to the doping of solid materials, depending on the objective of the treatment. The first is overall doping into a material in order to achieve functional improvements for the whole sample. The solid state reaction technique of heat-treating a mixture of dopant and target materials is an example of this. On the other hand, space-selective doping or compositional modification has recently received much attention for the fabrication of advanced inorganic materials. The functions or properties of the doped areas, in this case, are distinguishable from those of the overall matrix. In particular, this is an important process for the preparation of functional glass for optical applications such as photo-waveguides and micro-lens arrays. The ion-injection technique, using focused gas phase ions at low pressures,[14)] and the ion-exchange technique using molten[15)] salts are examples of this approach. Previous studies have substantiated the possibility of selectively inducing a change in the valence states of metal ions on a micrometer scale inside a glass sample by employing a focused laser.[16)–18)]

In contrast to the conventional approaches, we have proposed a new solid-state electrochemical route for pinpoint doping into desired locations within a glass or ceramics using an ion conductor.[9),19)] Figure 1(a) illustrates the basic cation migration mechanism for the pinpoint doping at the microcontact between metal ion conductor and doping target. Typically, pyramidal M-β''-Al_2O_3 (M = metal) ceramics was employed as an ion conductor at the anodic side. As well-known, the Na-β''-Al_2O_3 layered structure can substitute Na^+ for various kinds of alkaline, alkali earth, and heavy metal ions,[20),21)] and can behave as metal sources of these ions in the present system. Under applying a dc field at high temperature, Ag is electrochemically oxidized to Ag^+ at the Ag (anode) | M-β''-Al_2O_3 interface, and then M^{n+} is injected into the target material. Q^{m+} in the target is released to the Na-β''-Al_2O_3 (cathode side) for maintenance of electrical neutrality in the target material during the electrolysis. Na deposited at the Na-β''-Al_2O_3 | Ag (cathode) interface then immediately reacts with O_2 and CO_2 in the air to form Na_2CO_3.[22)] Consequently, M^{n+} is substituted for Q^{m+} under an electric field. Therefore, this doping scheme corresponds to an "*electrosubstitution*" mechanism.[23)] Since the contact radius between the M-β''-Al_2O_3 pyramid and doping target is small (~10 μm), we are able to demonstrate pinpoint doping into desired position in the target on a 10^1–10^2 μm scale using an ion conductor.

The pinpoint doping into alkali borosilicate glass was carried out using the proposed system. Glasses containing alkali metal cations are very useful as doping targets because these glasses show pure ionic conduction of the alkali metal cations. These cations in the glass are electrochemically substituted by the dopant. The feasibility of pinpoint doping strongly depended on the valence of the dopant cation. Monovalent cations (Ag^+, Li^+, etc.) could be easily doped into the glass. However, divalent cations such as Pb^{2+}, Zn^{2+}, Ca^{2+}, and Sr^{2+} could not be doped, because the divalent cation is more significantly affected than the monovalent cation by electrostatic interaction with the oxide ion in the glass. **Figure 3**(a) shows EPMA elemental maps for an anodic surface and cross section of Ag-doped glass with a Ag-β''-Al_2O_3 using the electrolysis system shown in Fig. 1(a). According to the elemental maps in the anodic surface, Ag was distributed in the manner of a circle drawn with its center at the microcontact. As expected, the characteristic X-ray intensity of alkali metal (Na) decreased at the area where Ag was detected. The elemental distributions of the other glass forming elements were not affected by electrolysis because the doping was carried

out below the glass transition temperature. These results indicate that Ag^+ is electrochemically substituted for Na^+ in the glass, and the ion migrations as noted above proceeded during the electrolysis. Judging from both maps in Fig. 3(a), Ag doping using the pyramid-like Ag-β''-Al_2O_3 resulted in a hemispherical dopant distribution centered on the microcontact between Ag-β''-Al_2O_3 and the glass. In general, metal ions would move in a perpendicular direction to equipotential surfaces during the electrolysis. Fleig et al. have reported that the equipotential surfaces between a micro- and a planar electrode exhibit a hemispherical shape with the center at the point of microcontact.[24),25)] Thus, it can be concluded that in the present study, Ag^+ diffused radially from the Ag-β''-Al_2O_3 | glass microcontact during doping. Consequently, a hemispherical distribution of silver was obtained. The diameter of the Ag-doped area in the glass depended on the applied electric charge which reflects the amount of Ag doping. Quantitative analysis revealed that the Ag doping into sodium borate glass proceeded with high current efficiency above 90%, which was estimated from the actual doping amount of Ag and applied electricity using Faraday's law.[26)] The facts support that the dopant amount and dispersion in glass can be tailored by varying the applied electric charge as well as the contact shape and/or size of the ion conductor.

With respect to the pinpoint doping into glasses, some interesting phenomena were caused during the pinpoint metal ion doping into the glasses. For instance, the detailed investigation of the electrosubstitution behavior of the mixed alkali glass (including Na^+ and K^+) by monovalent cation doping (Li^+, Ag^+, and Cs^+) revealed that the replaced alkali ion species were determined by the dopant types.[27)] That is, Li^+ ions attacked only Na^+ sites, and Ag^+ ions replaced Na^+ sites more readily than K^+. In contrast, Cs^+ ions simultaneously substituted for both Na^+ and K^+ sites. The observed electrosubstitution behaviors could be explained by the difference in ionic conductivity between Na^+ and K^+ and the radius of the dopant ions. In addition, it was substantiated that the solid electrochemical doping proposed here was effective for inhibiting crack development in the target glass which is frequently caused by high stress in the doped part.[28)]

Pinpoint metal ion doping into the superconducting ceramics was also performed using a M-β''-Al_2O_3.[19)] In this case, the electrosubstitution of dopant for Q^{m+} in the ceramics (Fig. 1(a)) was difficult because the ceramics shows pure electron conduction but no significant ionic conduction, in contrast to the glass containing an alkali metal. To overcome the problem, oxide ion conductor (yttria-stabilized zirconia) is used at the cathodic side instead of Na-β''-Al_2O_3 as shown in Fig. 1(b). In this case, M^{n+} and O^{2-} are simultaneously injected into the doping target under electric field. Therefore, this doping is called the "*electro-bi-injection*" mechanism.[29)] According to the elemental maps of the doped ceramics, the distribution of dopant occurred in a hemispherical shape in the same manner as the silver doping into glass, and the metal ions existed only into the grain boundaries of the ceramics on a micrometer scale. This may be based on the higher ionic mobility in the grain boundaries than that of the grain bulk even though the total ionic conductivity is small. Consequently, it was confirmed that the proposed technique is useful for pinpoint doping not only for glasses but also various ceramics.

Our method would conceivably enable micropatterning of dopants in target if the pyramidal M-β''-Al_2O_3 were to be moved along the target surface during doping.[30),31)] Hence, electrochemical design of silver distribution near the surface of the alkali borosilicate glass was also carried out using an equivalent electrolysis system to Fig. 1(a). As expected, scanning Ag-β''-Al_2O_3 tip under applying an electric field resulted in the fine-patterned Ag-distribution in the glass surface as shown in Fig. 3(b). The size and shape of these patterns could be easily controlled by adjusting electrolysis conditions. Since the Ag-β''-Al_2O_3 was attached to the automated XYZ stage, we could draw various silver patterns in the glass surface, not only simple structures (points and lines) but also more complicated forms. The lowest patterned Ag line width achieved to date is about 10 μm. However, the use of an ion conductor with a smaller contact radius and/or lower constant current (applied voltage) may enable the fabrication of finer patterns.

In summary, the pinpoint doping into the selected area of the solid target was accomplished using a metal ion conductor with a tiny contact area. The size and shape of dopant distribution could be easily controlled by adjusting electrolysis conditions. Although the ion injection technique makes selective patterning possible by focusing the ion beam, it requires high energy for ion acceleration in a vacuum system, and the doping occurs only in the surface region of the substrate.[32)] In contrast, the present technique allows single step fabrication of patterned glass since various forms can be drawn directly via the solid-solid interface under ambient atmosphere. A variety of metal ion conducting solid electrolytes has been developed to date. Thus, this method can be employed to introduce many different kinds of metal ions into solid target to impart it with new functions.

3. Solid state electrochemical micromachining

More recently, we proposed the micromachining technique of metal substrates through solid electrochemical reaction of metal ion conductors (Fig. 2(a)); the method was referred to as solid state electrochemical micromachining (SSEM).[10)] As is well known, conventional electrochemical micromachining (EM) works by the local anodic dissolution of a metal plate with or without masking in electrolyte solutions.[33)–36)] The related application of the electrochemical local etching of metal substrates covered with ion conducting polymers instead of electrolyte solutions have been studied by another group.[37),38)] In contrast, SSEM involves an anodic electrochemical reaction at the microcontact between the metal substrate and ion conductor. The proposed method has many advantages over other EM techniques: (1) no liquid electrolytes, which are difficult to handle, are required, (2) high-resolution direct structuring can be achieved without pretreatments such as masking or coating, (3) the shape of the apex of an ion conductor can be transferred to the metal surface. Of course, the advantages of conventional EM, including simplicity of the apparatus and fine-tunability of etching rate and/or size through optimization of electrochemical parameters, are valid in the case of SSEM as well.

Figure 2(a) depicts the model for ion migration using a metal ion conductor. Even though the electrolysis system is similar to that for the pinpoint doping, the ion conductor is placed at the cathodic side. The solid state electrochemical cell consists of a metal substrate (anode M = Ag, Cu, Zn) | pyramidal Na-β''-Al_2O_3 | Ag plate (cathode) system. That is, SSEM utilizes an ion conductor instead of the solution electrolyte used in conventional EM. As stated already, the Na-β''-Al_2O_3 structure can substitute Na^+ for various kinds of alkaline, alkali earth, and heavy metal ions. Thus, Na-β''-Al_2O_3 seems appropriate as an ion conductor for SSEM. Under an applied electric field, the metal substrate is electrochemically oxidized to metal ions (M^{n+}) at the M | Na-β''-Al_2O_3 microcontact and these M^{n+} ions migrate into the Na-β''-Al_2O_3. As a result of continuous electrolysis, the metal substrate

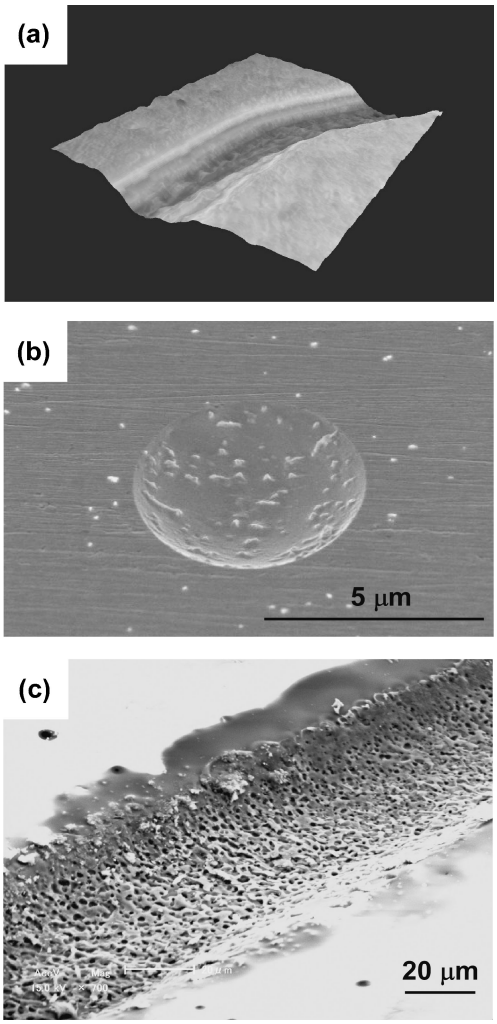

Fig. 4. (a) 3D profile of Ag surface after SSEM after scanning Na-β''-Al_2O_3 (0.01 mm/s) at 873 K and 20 μA. The depth and width of track produced by the SSEM were about 10 and 55 μm, respectively. (b) SEM image of Ag surface after micromachining at 1 nA for 5 min using Nafion coated tungsten microelectrode, where the electrolysis was carried out at room temperature. (c) Line-patterned β-SiC surface after applying 10 V for 5 h at 1423 K using NiO-added YSZ.

was locally consumed at the microcontact, and thus the SSEM is accomplished. In fact, various metal substrates (Ag, Cu, and Zn) could be grooved using the Na-β''-Al_2O_3 pyramid,[39] where the metal ions eliminated from the substrate were detected in the cross section of the Na-β''-Al_2O_3. Thus, the ion migration mechanism proposed above actually proceeded during the electrolysis. It was confirmed that the machining size or depth depended on the electrolysis conditions (current, operating time) and the apex configuration of Na-β''-Al_2O_3. In addition, the scanning of the Na-β''-Al_2O_3 pyramid during electrolysis produced a fine patterned metal substrate in the same manner as the pinpoint doping (**Fig. 4**(a)). However, the current efficiencies of the SSEM (~40%), which were calculated from the machining volume, applied electricity, and density of metal using Faraday's law, were relatively low as compared with the pinpoint doping, indicating that the decomposition of β''-Al_2O_3 crystals and the subsequent electron conduction through the cell proceeded under applying a local high electric field at the microcontact.

In the case of the SSEM employing Na-β''-Al_2O_3, the reproducible fabrication of β''-Al_2O_3 having a sharp apex was difficult because Na-β''-Al_2O_3 is a hard ceramic material. Thus, the resolution of solid electrochemical micromachining was poor (10^1–10^2 μm). Moreover, as Na-β''-Al_2O_3 attains high ion conductivity only at high temperature (~600°C), micromachining had to be performed at this temperature range. In order to solve these problems including the low current efficiency, the SSEM was performed using an ion conducting polymer in place of a Na-β''-Al_2O_3. As is well known, Nafion has high proton conductivity even at room temperature and no anisotropic conduction. Additionally, a variety of metal ions can travel in hydrophilic cation conduction channels instead of protons.[40] This allows solid state electrochemical micromachining of various metals under mild conditions (room temperature). Hence, the SSEM of various metal plates (Ag, Cu, Zn, Mg, and Fe) was attempted using Nafion coated tungsten microelectrode.[41] In general, metals can be easily oxidized at high temperature in an oxidizing atmosphere, whereby a thick oxide film is formed on surface. In the case of micromachining using Na-β''-Al_2O_3 at high temperature, the presence of the oxide film suppresses the anodic dissolution of metal, and an inert atmosphere is required to prevent surface oxidation. Also, metals having a low melting temperature could not be employed as a target of micromachining. Owing to the high ion conductivity of Nafion even at room temperature, various kinds of metals can be used as a target without the restrictions mentioned above. As a result, all metal substrates investigated (Ag, Cu, Zn, Mg, and Fe) were dissolved locally and anodically at the microcontact with the ion conducting Nafion (Fig. 4(b)). By coating a W microelectrode with Nafion, the apex shape of a Nafion layer could be transferred directly to the metal surface without any detectable side etching or expansion of machining dimensions. In addition, the accuracy of machining (submicron scale) was improved as compared with the SSEM using Na-β''-Al_2O_3, and room-temperature operation was achieved. While the formation of a surface oxide caused a significant current loss in some cases, the maximum current efficiency (ca. 70%) of the Nafion-induced SSEM was much higher than that obtained using β''-Al_2O_3.

In a similar manner to the SSEM of metal substrate, the electrochemical micromachining of materials producing volatile substances by oxidation could be achieved using an oxide ion conductor (Fig. 2(b)).[42] Such a novel application may extend the possibilities of oxide ion conductors. The hard materials such as carbon based ceramics (glassy carbon, SiC, and WC) or hard metals (W and Mo) were appropriate targets for the proposed technique, because these non-oxide materials form gaseous or volatile oxidation products. The modified solid electrochemical cell exploits a pyramid-like oxide ion conducting ceramics instead of β''-Al_2O_3 as shown in Fig. 2(b). Application of a dc bias to the cell induces the anodic electrochemical reaction of O^{2-} at the microcontact between the conductor and the target. When the target forms volatile or gaseous products as a result of the reaction with O^{2-} or O_2 gas, it is expected that the target is gradually consumed during the electrolysis. In the present solid state cell for the SSEM, yttria stabilized zirconia ceramics (YSZ) containing a small amount of NiO was selected as the oxide ion conductor. The ceramic or pure metal plates of glassy carbon (GC), WC, β-SiC, W, and Mo were used as workpieces for the SSEM. The reaction of the oxide ions with the GC surface via the microcontact successfully led to a local etching (surface micromachining) accompanied by the CO_2(g) generation in the inert N_2 atmosphere. On the other hand, the possibility of the SSEM of

β-SiC ceramics strongly depended on the operation temperature and partial pressure of oxygen (p_{O2}) around the microcontact that is roughly controlled by the electrolysis current. While the passive oxidation forming SiO_2(s) dominated at low temperature and high partial pressure of oxygen (p_{O2}), the depression of the β-SiC surface was fabricated by the SSEM at high temperature and low p_{O2} condition. According to microscopic observation of the latter sample, the numerous tiny pores with a few microns in diameter were discernible in the etched surface (Fig. 4(c)). The porous surface is one of the characteristics of active oxidation and seems to be produced by simultaneous evaporation of SiO and CO.[43] Moreover, it was confirmed that the surface micromachining of W and Mo was also possible by local oxidation at high temperature using the present method. These results could be explained that the local area of W or Mo substrate was selectively scratched as a result of the oxidation with O^{2-} and/or O_2, and subsequent sublimation of the produced oxides, i.e., WO_3 (>1100 K) and MoO_3 (>973 K). Consequently, it was demonstrated that a selective oxidation of the non oxide plates by the oxide ion conductor realizes the local consumption i.e., surface etching. As a matter of course, the advantages of the SSEM, including easy control of machining size and three dimensional microstructure, are also valid in the case of SSEM using an oxide ion conductor. On the other hand, it should be noted that the present technique has some disadvantages such as the relative coarse machining accuracy, the slow etching rate, and requirement of high temperature or inert atmosphere. Therefore, in the future, these problems will be solved by use of oxide ion conductor driving even at lower temperatures.

In this section, it was demonstrated that the anodic reaction at the microcontact of metal or oxide ion conductor enables solid state electrochemical micromachining of metal or ceramics surfaces. It is considered that the present method can extend to fabricate a variety of machining patterns, including not only simple patterns, but also more complex structures. In conventional EM in solution electrolyte, the machining size is always larger than that of the counter electrode because the presence of the electrolyte solution even if the metal surface is covered with a masking layer. Moreover, the impregnation of the electrolyte solution under the mask causes a spread in the machining dimension. In contrast, since the solid state technique utilizes direct ion migration via a solid–solid microcontact, the machining dimension is almost identical to the apparent contact size, which means that the desired aspect ratio of machining can be easily yielded. Furthermore, the electrochemical technique enables micromachining without any mechanical stress or distortion to the substrate. In the near future, therefore, the present technique is expected to be recognized as one of most important surface microstructuring methods.

4. Conclusions

The present contribution summarized the original applications of ion conductors which employ ion migration through the microcontact of ion conductors. Such new applications could be developed by simple reduction of contact area as compared to conventional planar contact without finding any new theory or phenomenon. While the resolution of the present microfabrication techniques is not sufficient for achieving the nanosized resolution at present, advances of microcontact fabrication and selection of appropriate ion conductor will improve the accuracy of pinpoint doping or micromachining. Scanning probe microscopy may be a useful tool to construct a minute solid-solid contact on nanoscale. Hence, the success of the proposed method based on novel aspects of the ion conductors may stimulate conventional applications of ion conductors.

Acknowledgements The author is deeply grateful to Prof. Yasumichi Matsumoto of Kumamoto University and Profs. Naoya Enomoto and Junichi Hojo of Kyushu University for their kind assistances and valuable discussions on the present study.

References

1) J. Fleig, *Solid State Ion.*, **161**, 279–289 (2003).
2) J. Fleig, S. Rodewald and J. Maier, *Solid State Ion.*, **136–137**, 905–911 (2000).
3) H.-D. Wiemhöfer, *Ber. Bunsenges. Phys. Chem*, **97**, 461–469 (1993).
4) W. Zipprich, S. Waschilewski, F. Rocholl and H.-D. Wiemhöfer, *Solid State Ion.*, **101–103**, 1015–1023 (1997).
5) G. Fafilek, *Solid State Ion.*, **113–115**, 623–629 (1998).
6) G. Fafilek and S. Harasek, *Solid State Ion.*, **119**, 91–96 (1999).
7) H. Rickert and H.-D. Wiemhöfer, *Ber. Bunsenges. Phys. Chem*, **87**, 236–239 (1983).
8) S. Lübke and H.-D. Wiemhöfer, *Solid State Ion.*, **117**, 229–243 (1997).
9) K. Kamada, S. Udo and Y. Matsumoto, *Electrochem. Solid-State Lett.*, **5**, J1–J3 (2002).
10) K. Kamada, K. Izawa, Y. Tsutsumi, S. Yamashita, N. Enomoto, J. Hojo and Y. Matsumoto, *Chem. Mater.*, **17**, 1930–1932 (2005); *Correction*, **18**, 1713 (2006).
11) A. Spangenberg, J. Fleig and J. Maier, *Adv. Mater.*, **13**, 1466–1468 (2001).
12) K. Terabe, T. Nakayama, T. Hasegawa and M. Aono, *Appl. Phys. Lett.*, **80**, 4009–4011 (2002).
13) K. Terabe, T. Nakayama, T. Hasegawa and M. Aono, *J. Appl. Phys.*, **91**, 10110–10114 (2002).
14) M. Antonello, G. W. Arnold, G. Battaglin, R. Bertoncello, E. Cattaruzza, P. Colombo, G. Mattei, P. Mazzoldi and F. Trivillin, *J. Mater. Chem.*, **8**, 457–461 (1998).
15) M. A. Villegas, J. M. Fernandez Navarro, S. E. Paje and J. Llopis, *Phys. Chem. Glasses*, **37**, 248–253 (1996).
16) J. Qiu, C. Zhu, T. Nakaya, J. Si, K. Kojima, F. Ogura and K. Hirao, *Appl. Phys. Lett.*, **79**, 3567–3569 (2001).
17) K. Miura, J. Qiu, S. Fujiwara, S. Sakaguchi and K. Hirao, *Appl. Phys. Lett.*, **80**, 2263–2265 (2002).
18) J. Qiu, M. Shirai, T. Nakaya, J. Si, X. Jiang, C. Zhu and K. Hirao, *Appl. Phys. Lett.*, **81**, 3040–3042 (2002).
19) K. Kamada, S. Udo, S. Yamashita and Y. Matsumoto, *Solid State Ion.*, **146**, 387–392 (2002).
20) J. L. Briant and G. C. Farrington, *J. Solid State Chem.*, **33**, 385–390 (1980).
21) G. C. Farrington and B. Dunn, *Solid State Ion.*, **7**, 267–281 (1982).
22) Y. Matsumoto, K. Akagami and K. Kamada, *J. Solid State Chem.*, **143**, 111–114 (1999).
23) Y. Matsumoto, *Solid State Ion.*, **100**, 165–168 (1997).
24) J. Fleig and J. Maier, *Electrochim. Acta*, **41**, 1003–1009 (1996).
25) J. Fleig, P. Pham, P. Sztulzaft and J. Maier, *Solid State Ion.*, **113–115**, 739–747 (1998).
26) K. Kamada, S. Udo, S. Yamashita, Y. Tsutsumi and Y. Matsumoto, *Solid State Ion.*, **160**, 389–394 (2003).
27) K. Kamada, Y. Tsutsumi, S. Yamashita and Y. Matsumoto, *J. Solid State Chem.*, **177**, 189–193 (2004).
28) K. Kamada, K. Izawa, S. Yamashita, Y. Tsutsumi, N. Enomoto, J. Hojo and Y. Matsumoto, *Solid State Ion.*, **176**, 1073–1078 (2005).
29) K. Kamada and Y. Matsumoto, *J. Solid State Chem.*, **146**, 406–410 (1999).
30) K. Kamada, S. Yamashita and Y. Matsumoto, *J. Mater. Chem.*, **13**, 1265–1268 (2003).

31) K. Kamada, S. Yamashita and Y. Matsumoto, *J. Electrochem. Soc.*, 151, J33–J37 (2004).
32) G. W. Arnold and J. A. Borders, *J. Appl. Phys.*, 48, 1488–1496 (1977).
33) P.-F. Chauvy, P. Hoffmann and D. Landolt, *Electrochem. Solid-State Lett.*, 4, C31–C34 (2001).
34) E. J. Teo, M. B. H. Breese, E. P. Tavernier, A. A. Bettiol, F. Watt, M. H. Liu and D. J. Blackwood, *Appl. Phys. Lett.*, 84, 3202–3204 (2004).
35) R. Schuster, V. Kirchner, P. Allongue and G. Ertl, *Science*, 289, 98–101 (2000).
36) P. Allongue, P. Jiang, V. Kirchner, A. L. Trimmer and R. Schuster, *J. Phys. Chem. B*, 108, 14434–14439 (2004).
37) O. E. Hüsser, D. H. Craston and A. J. Bard, *J. Vac. Sci. Technol., B*, 6, 1873–1876 (1988).
38) O. E. Hüsser, D. H. Craston and A. J. Bard, *J. Electrochem. Soc.*, 136, 3222–3229 (1989).
39) K. Kamada, M. Tokutomi, N. Enomoto and J. Hojo, *Electrochim. Acta*, 52, 3739–3745 (2007).
40) N. Yoshida, T. Ishisaki, A. Watakabe and M. Yoshitake, *Electrochim. Acta*, 43, 3749–3754 (1998).
41) K. Kamada, M. Tokutomi, M. Inada, N. Enomoto and J. Hojo, *J. Ceram. Soc. Jpn.*, 115, 672–677 (2007).
42) K. Kamada, S. Hirata, N. Enomoto and J. Hojo, *Solid State Ion.*, 180, 1226–1230 (2009).
43) T. Goto, *J. Ceram. Soc. Jpn.*, 110, 884–889 (2002).

Kai Kamada received his PhD degree from Kumamoto University in 2003. He was a research associate of Department of Applied Chemistry and Biochemistry, Kumamoto University in 1999–2004 and Department of Applied Chemistry, Kyushu University in 2004–2007. Since 2008, he has been working at Department of Materials Science and Engineering, Nagasaki University as an assistant professor. His current research interest has been devoted to solid-state or photoelectrochemical fabrication of inorganic functional materials.